International Dairy Journal 20 (2010) 79–88

Contents lists available at ScienceDirect

International Dairy Journal

journal homepage: www.elsevier.com/locate/idairyj

Casein glycomacropeptide pH-dependent self-assembly and cold gelation

M.E. Farías [a,b], M.J. Martinez [a], A.M.R. Pilosof [b,*]

[a] Departamento de Industrias, Facultad de Ciencias Exactas y Naturales, Universidad de Buenos Aires, Ciudad Universitaria (1428), Buenos Aires, Argentina
[b] Departamento de Tecnología, Universidad Nacional de Luján, Ruta 5 y 7, Luján (6700), Buenos Aires, Argentina

ARTICLE INFO

Article history:
Received 3 July 2009
Received in revised form
11 September 2009
Accepted 13 September 2009

ABSTRACT

The self-assembly of 3–5% (w/w) casein glycomacropeptide (CMP) at room temperature and pH 3–6.5 was determined by dynamic light scattering immediately after pH adjustment and over time, and the rate of gelation at a concentration of 3–10% (w/w) was determined by a tilting test. The intensity particle size distribution at pH 6.5 was multimodal with a predominant peak at 2.3 nm. The hydrodynamic diameter increased when decreasing the pH from 6.5 to 3. CMP solutions at a pH below 4.5 showed time-dependent self-assembly at room temperature, which led over time to gelation. The minimum concentration for cold gelation depended on pH. Below pH 4, CMP gelled even at low concentrations (3%, w/w). The pH-reversibility of self-assembled CMP was not total, showing that hydrophobically bound dimers, once formed, are stable to pH changes. A model to explain CMP self-assembly and the formation of a network-like structure (gel) at room temperature is proposed.

1. Introduction

Casein glycomacropeptide (CMP) is released after specific cleavage of κ-casein by chymosin or pepsin at the Phe_{105}-Met_{106} peptide bond (Daali, Cherkaoui, & Veuthey, 2001; Kawasaki et al., 1993; Thomä-Worringer, Sørensen, & López Fandiño, 2006). CMP comprises the 64 amino acids in the hydrophilic C-terminal portion of κ-casein, and contains all the posttranslational modifications (glycosylation and phosphorylation) present in κ-casein that contribute to its marked heterogeneity (Mikkelsen et al., 2005).

Next to β-lactoglobulin (β-lg), α-lactalbumin (α-la), and bovine serum albumin, CMP is the most abundant protein/peptide in whey products (whey protein concentrate, WPC, and whey protein isolate, WPI) manufactured from cheese whey; typical concentrations are between 20 and 25% of the proteins (Thomä-Worringer et al., 2006; Wang & Lucey, 2003).

In recent years, CMP has been the subject of growing interest due to its beneficial biological and physiological properties including the ability to bind cholera and *Escherichia coli* enterotoxins, inhibit bacterial and viral adhesion, modulate immune systems responses, promote bifidobacterial growth, suppress gastric secretions and regulate blood circulation, as reviewed by El-Salam, El-Shibiny, and Buchheim (1996) and Thomä-Worringer et al. (2006). The biological activities are mainly attributed to the carbohydrate chains. CMP has an amphiphilic nature, which results from a partial glycosylation. The sugar residues are highly hydrophilic, whereas the peptide chain is more hydrophobic (Tolkach & Kulozik, 2005).

Glycosylated forms of CMP (gCMP) represent about 50% of the total CMP (Mollé & Leonil, 2005). Different O-glycosylation sites as well as oligosaccharide chains made of one or more of the *N*-acetylneuraminic (sialic) acid, galactose and *N*-acetylgalactosamine residues have been identified in CMP (Daali et al., 2001). The most predominant carbohydrate is sialic acid (Coolbear, Elgar, & Ayers, 1996). Sialic acid was found to be particularly important for the biological and pharmacological activity of glycoproteins and in some cases, its loss causes reduced activity (Daali et al., 2001). It is an acidic sugar with a pKa value of 2.2. A higher concentration of sialic acid in CMP gives a lower pI for this glycopeptide. The precise pI of CMP is dependent on the nature and content of the attached sialylated carbohydrate chains and/or on the degree of phosphorylation (Cherkaoui, Doumenc, Tachon, Neeser, & Veuthey, 1997; Kreuβ, Krause, & Kulozik, 2008; Lieske, Konrad, & Kleinschmidt, 2004b; Nakano & Ozimek, 2000; Silva-Hernández, Nakano, & Ozimek, 2002).

The non-glycosylated CMP (aCMP) has a molecular mass between 6787 and 6755 Da depending on the genetic variant. The average molecular mass of total CMP is about 7500 Da with the highest mass of up to 9631 corresponding to highly glycosylated CMP (gCMP) (Mollé & Leonil, 2005). There is a general agreement that CMP behaves as a much larger peptide than its theoretical mass. Kawasaki et al. (1993) reported a pH-dependent association/dissociation of CMP. This apparent pH-dependent aggregation, however, is still debated (El-Salam et al., 1996; Thomä-Worringer et al., 2006)

* Corresponding author. Tel.: +54 11 45763377; fax: +54 11 45763366.
E-mail address: apilosof@di.fcen.uba.ar (A.M.R. Pilosof).

0958-6946/$ – see front matter © 2009 Elsevier Ltd. All rights reserved.
doi:10.1016/j.idairyj.2009.09.002

and in some studies, pH-dependent changes of the mass of CMP have not been observed (Lieske, Konrad, & Kleinschmidt, 2004a; Mikkelsen et al., 2005; Nakano & Ozimek, 1998).

Dynamic light scattering (DLS) is being increasingly used to determine molecular size, hydrodynamic radius and kinetics of aggregation of biopolymers. Proteins, owing to the special features of their molecular structure (a large number of both the polar and non-polar functional groups in their molecules), are prone to pronounced self-assembly in an aqueous medium as a result of weak physical bond formation, the character of which is varies markedly by the environmental conditions, such as acidification, addition of divalent ions or low-molecular mass ingredients, temperature or high-pressure treatment, fermentation (Semenova, 2007). In recent years, DLS has been used for studying the aggregation of β-lactoglobulin, α-lactalbumin, caseins and other proteins (Baeza, Gugliotta, & Pilosof, 2001; Elofsson, Dejmek, & Paulsson, 1996; Guyomarc'h, Nono, Nicolai, & Durand, 2009; Harnsilawat, Pongsawatmanit, & McClements, 2006; Hoffmann, Roefs, Verheul, Van Mil, & De Kruif, 1996; Karlsson, Ipsen, Schrader, & Ardö, 2005; McGuffey, Otterb, van Zantenc, & Foegeding, 2007; Mehalebi, Nicolai, & Durand, 2008; Roefs & De Kruif, 1994; Sharma, Haque, & Wilson, 1996). However, studies on CMP aggregation by this technique have not been reported. Therefore, the aim of present work was to study the kinetics of pH-dependent CMP self-assembly by DLS and its spontaneous cold gelation.

2. Materials and methods

2.1. Materials

Two commercial products of CMP were provided by two international suppliers and referred to as A and B for reasons of confidentiality. The declared CMP content was (dry basis): 90% (w/w) and 68% (w/w) for A and B, respectively.

CMP solutions were prepared freshly by dissolving the proper amount of powder in Milli-Q ultrapure water at room temperature and stirring for 30 min. Bulk concentrations of the CMP solutions were 3 and 5% (w/w) for DLS studies and 3–10% (w/w) for the tilting test (see Section 2.4). To prevent bacterial growth, 0.02% (w/w) NaN_3 was added to each sample. The pH was adjusted from 3 to 8 with HCl or NaOH of high molarity to limit dilution, and the ionic strength was kept below 4 mM. All solutions were filtered through a 0.45, 0.22 and 0.02 μm microfilter Whatman International Ltd. (Maidstone, England) before use.

2.2. Electrophoresis

Whey proteins were analyzed by one-dimensional SDS–PAGE-electrophoresis using a Mini-Protean II dual slab cell system (Bio-Rad Laboratories, Hercules, CA, USA) in dissociating conditions (2%, w/w, SDS) according to the procedure of Laemmli (1970). The resolving and stacking gels contained 12 and 4.5% (w/w) acrylamide, respectively. WPI (Arla Foods Ingredients, Viby J., Denmark), α-la enriched WPC (Arla Foods Ingredients, 88% dry basis), β-lg (Davisco Foods International, Le Sueur, MN, USA, 97.8% dry basis), A and B CMP samples were diluted in Milli-Q deionised water to 0.2% and then mixed (1:4) with the sample buffer (pH 6.8, 0.5 M Tris–HCl and glycerol with SDS) in the presence of β-mercaptoethanol as a reducing agent. Two gels were prepared at the same time. The weight of deposited protein was 40 μg per lane. Mixed Tris–HCl (0.4 M) glycine with SDS in distilled water solution to pH 8.3 was the running buffer. Proteins were stained with Coomassie Brilliant Blue (CBB) solution (0.1%, w/w) and destained with a mixture 1:1 of methanol-glacial acetic acid, 20% (w/w) (Bollag & Edelstein, 1991). The duration of this procedure was approximately 45 min. Protein standards from Bio-Rad were also used.

2.3. CMP self-assembly

CMP self-assembly at room temperature was determined by DLS in a Zetasizer Nano-Zs, Malvern Instruments (Malvern, England) provided with a He-Ne laser (633 nm) and a digital correlator, Model ZEN3600. Measurements were carried out at a fixed scattering angle of 173°, with a measurement range of 0.6 nm–6 μm according to the manufacturer. Samples were placed in a disposable polystyrene cell.

The particles are constantly moving due to Brownian motion, which is due to the random collision with the molecules of the liquid that surrounds the particle. Small particles move quickly and large particles move more slowly. In DLS, the sample is illuminated with a laser beam and the intensity of the resulting scattered light is dependent on the particle size because of the intensity fluctuations. The relationship between the size of the particle and the diffusion coefficient is defined by the Stokes–Einstein equation:

$$\mathrm{d}(H) = \frac{kT}{3\pi\eta D} \quad (1)$$

where, d(H): hydrodynamic diameter (m); D: translational diffusion coefficient ($m^2\,s^{-1}$); k: Boltzmann's constant ($1.38 \times 10^{-23}\,N\,m\,K^{-1}$); T: absolute temperature (K); η: solvent viscosity ($N\,s\,m^{-2}$).

Two approaches were utilized to obtain size information. Firstly, Contin's algorithm was used to analyze the data for percentile distribution of particle/aggregate sizes (Stepanek, 1993). The size distribution obtained is a plot of the relative intensity of light scattered by particles in various size classes and it is therefore known as an intensity size distribution. Although the fundamental size distribution generated by DLS is an intensity distribution, this can be converted, using Mie theory, to volume distribution. Secondly, a cumulant method was used to find the mean average (z-average) or the size of a particle that corresponded to the mean of the intensity distribution, and also the polydispersity index as an indicator of the degree of aggregation. The z-average is useful when citing a single average value for the purpose of comparison, but clearly inadequate for giving a complete description of the distribution results in polydisperse systems. The assay was carried out in triplicate.

2.4. Sol–gel transition

The sol–gel transition was determined by a modified tilting test (Relkin, Meylheuc, Launay, & Raynal, 1998). Tubes (4 mL capacity), containing 2 g of CMP solutions were observed over time (h or days) at 25 °C. The tubes were tightly closed to prevent water evaporation. The gelation time (t_{til}) was assumed to be reached when there was no deformation of the meniscus upon tilting. The gelation rate (V_{til}) was calculated as $1/t_{til}$. The reported values are the average of two or three replicates. The standard error of the mean was less than 10%.

3. Results and discussion

3.1. Electrophoretic profile of CMP

Whey proteins (WPI, β-lg, α-la, A CMP and B CMP) were examined using SDS–PAGE and the protein profiles are shown in Fig. 1. The pattern of WPI (lane B) presented several bands, with the predominant bands corresponding to the main components of WPI: β-lg (18.3 kDa) and α-la (14.2 kDa). Lanes C and D showed the

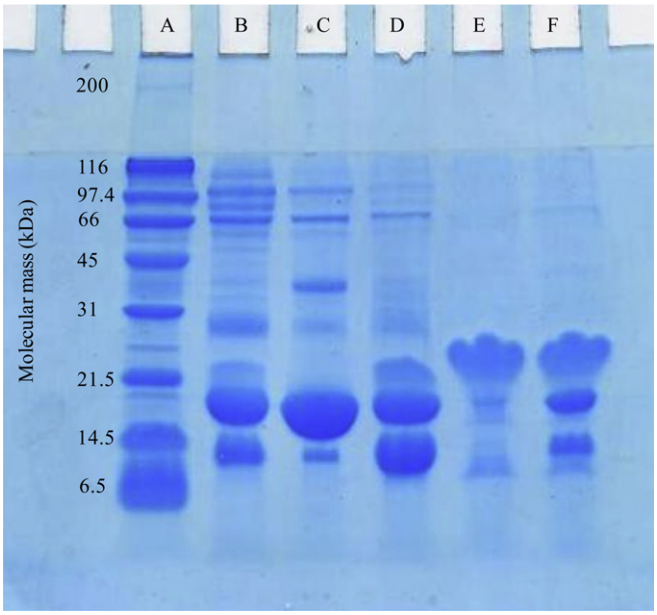

Fig. 1. SDS–PAGE patterns of: A) Molecular mass protein standards, B) whey protein isolate (WPI; Arla Foods Ingredients), C) β-lg (Davisco Foods International), D) α-la (Arla Foods Ingredients), E) A CMP and F) B CMP.

pattern of β-lg and α-la respectively, both of them corresponding to the monomeric forms. It is possible to observe the presence of important amounts of other WPI proteins in the pattern of α-la (i.e. β-lg). Analysis of A and B CMP by SDS–PAGE (lanes E and F respectively) gave minor and major broad bands stained with Coomassie Blue (CB). The major irregular band had a mass of 23–28 kDa, corresponding to aggregated forms of CMP (Nakano, Ikawa, & Ozimek, 2007; Silva-Hernández et al., 2002; Silva-Hernández, Nakano, Verdalet-Guzmán, & Ozimek, 2004), whereas a minor band was located between aprotinin (6.5 kDa) and lysozyme (14.4 kDa), corresponding to monomeric CMP form. This minor band was visible in both A and B CMP with weak staining. B CMP also showed the greater presence of other whey proteins (β-lg and α-la) reflecting its low purity compared with A CMP. The location of the major band of CMP immediately following the β-lg is consistent with the previously reported SDS–PAGE pattern (Morr & Seo, 1988). The major band was not regularly stained with CB. The broadness and irregularity of this band has been attributed to variations in the glycosylation degree of CMP (Nakano & Ozimek, 2000; Silva-Hernández et al., 2002). Nakano et al. (2007) analyzed the sialic acid contained in each protein fraction following SDS–PAGE-electrophoresis of A CMP. They found that sialic acid was present in the major irregular broad stained band in lane E (Fig. 1) but it was also present in a non-stained area with lower mobility, above the major stained band. In addition, Nakano et al. (2007) have shown that only a small amount of sialic acid was detected in the areas where most of the CBB-staining bands were seen in cellulose acetate electrophoresis of CMP. In contrast most (~70%) of sialic acid in A CMP was found in the area corresponding to the fastest weak CB-stained band. It appears that CMP with negatively charged sialic acid and phosphate has a low affinity to CBB having a negative charge (Nakano et al., 2007), so that CBB staining in SDS–PAGE gel would not detect most of sialylated CMP.

Considering that the molecular mass of the maximum glycosylated form of gCMP is about 11 kDa (Kreuß, Strixner, & Kulozik, 2009) and of aCMP is 7 kDa, the broad irregular band between 23 and 28 kDa in Fig. 1 could consist of different hydrophobically associated forms of tetrameric aCMP or dimeric gCMP, probably formed during cheese-making or processing of CMP. Nevertheless they were present together with monomeric forms of CMP not revealed by staining with CBB. Monomeric CMP would also be washed out of the gel, which will further reduce the amount of detected CMP. Therefore the actual concentration of monomeric sialylated CMP would be much greater than is apparent based on the density of the bands in SDS–PAGE analysis (Etzel, 1999).

3.2. Particle size distribution of CMP at its original pH (6.5)

The intensity size distribution of 5% (w/w) CMP at pH 6.5 is shown in Fig. 2A, indicating three size populations for A CMP. The hydrodynamic diameter, d(*H*), of the predominant lower size peak in A CMP size distribution at pH 6.5 was found to be between 1 and 5 nm with the maximum peak at 2.5 nm. A rough estimate of the molecular mass of CMP with the Zetasizer Nano-Zs software, for globular proteins, indicated that the monomeric form of CMP (average about 7500 Da) should have a size of approximately 2.6 nm. This prediction should be treated with some caution because this estimation is for globular proteins, and CMP is not

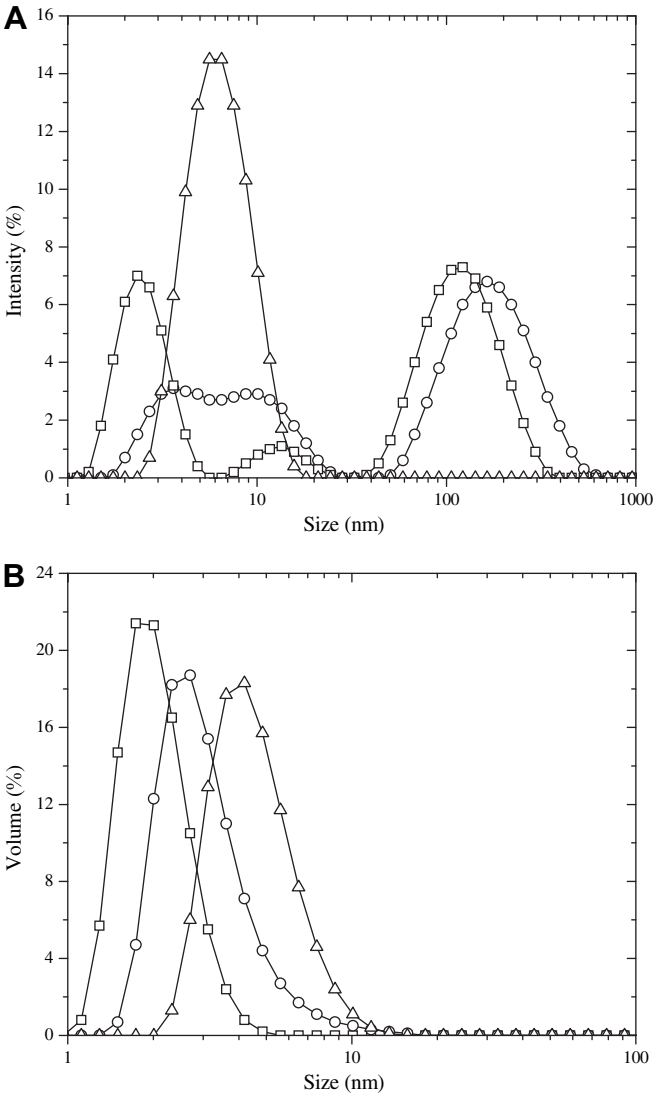

Fig. 2. (A) Intensity and (B) volume size distribution at pH 6.5 and 25 °C for 5% (w/w) CMP solutions: (□) A CMP, (○) B CMP. For comparison a 5% (w/w) β-lg solution is included (△).

a globular protein. Aggregates of approximate size 15 and 100 nm were also apparent in the A CMP intensity distribution, but their number was negligible as can be deduced from the volume size distribution plots (Fig. 2B). Therefore, in A CMP at pH 6.5 the monomeric form predominated together with more aggregated forms like dimers, trimers and tetramers that would have a d(H) of within 3.5 and 5 nm. The DLS results are in accordance with the electrophoretic results showing two main forms of CMP, but differ in the fact that PAGE-electrophoresis reveals that the associated forms are predominant because of a low affinity of CB for sialylated CMP. Using electrophoretic techniques, Silva-Hernández et al. (2002) showed that the majority of goat CMP contains at least two separate components: one that does not dissociate and other that dissociates in the presence of SDS, but the latter is the minor component. However, it would be possible that the dissociated forms of CMP reported by Silva-Hernández et al. (2002) and in Fig. 1 are not the minor components but are a result of less CBB staining intensity compared with the associated form, as discussed above.

The lower size peak of B CMP in Fig. 2 A corresponded to slightly higher d(H) values than A CMP, broadening from 2 to 20–25 nm where the monomeric form was not apparent. This size distribution could be related to the presence of other whey proteins, mainly β-lg in B CMP as has been shown in Fig. 1. In previous work, the existence of associative interactions between CMP and β-lg in the aqueous phase at neutral pH has been demonstrated by DLS, differential scanning calorimetry (DSC), fluorometry and native PAGE-electrophoresis (Martínez, Carrera Sánchez, Rodríguez Patino, & Pilosof, 2009). In fact, the results obtained by DLS showed

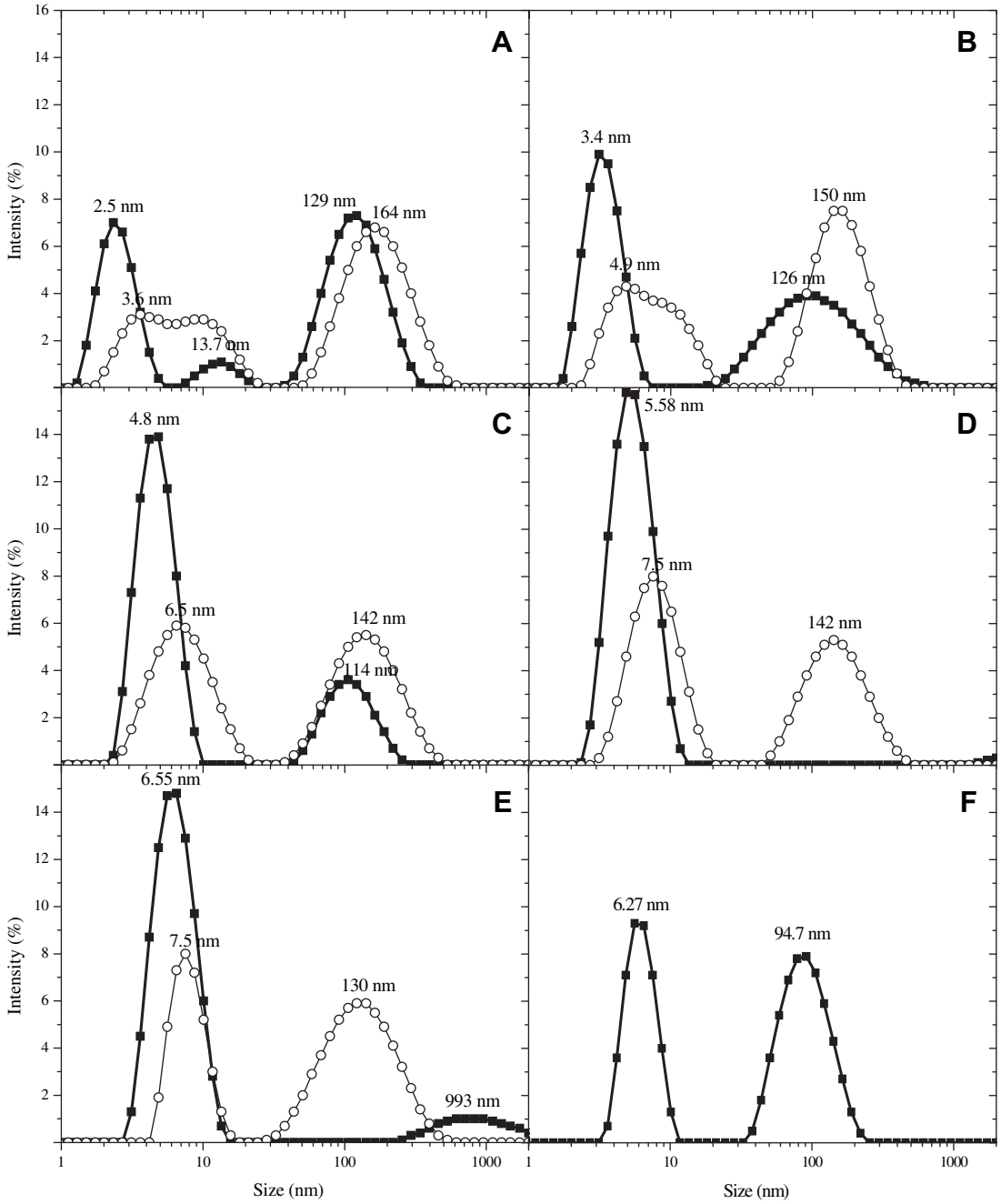

Fig. 3. Intensity size distribution at 25 °C for CMP solutions at 5% (w/w) from (■) A and (○) B immediately after pH adjustment: (A) pH 6.5; (B) pH 5.5; (C) pH 5; (D) pH 4.5; (E) pH 3.5 and (F) pH 3.

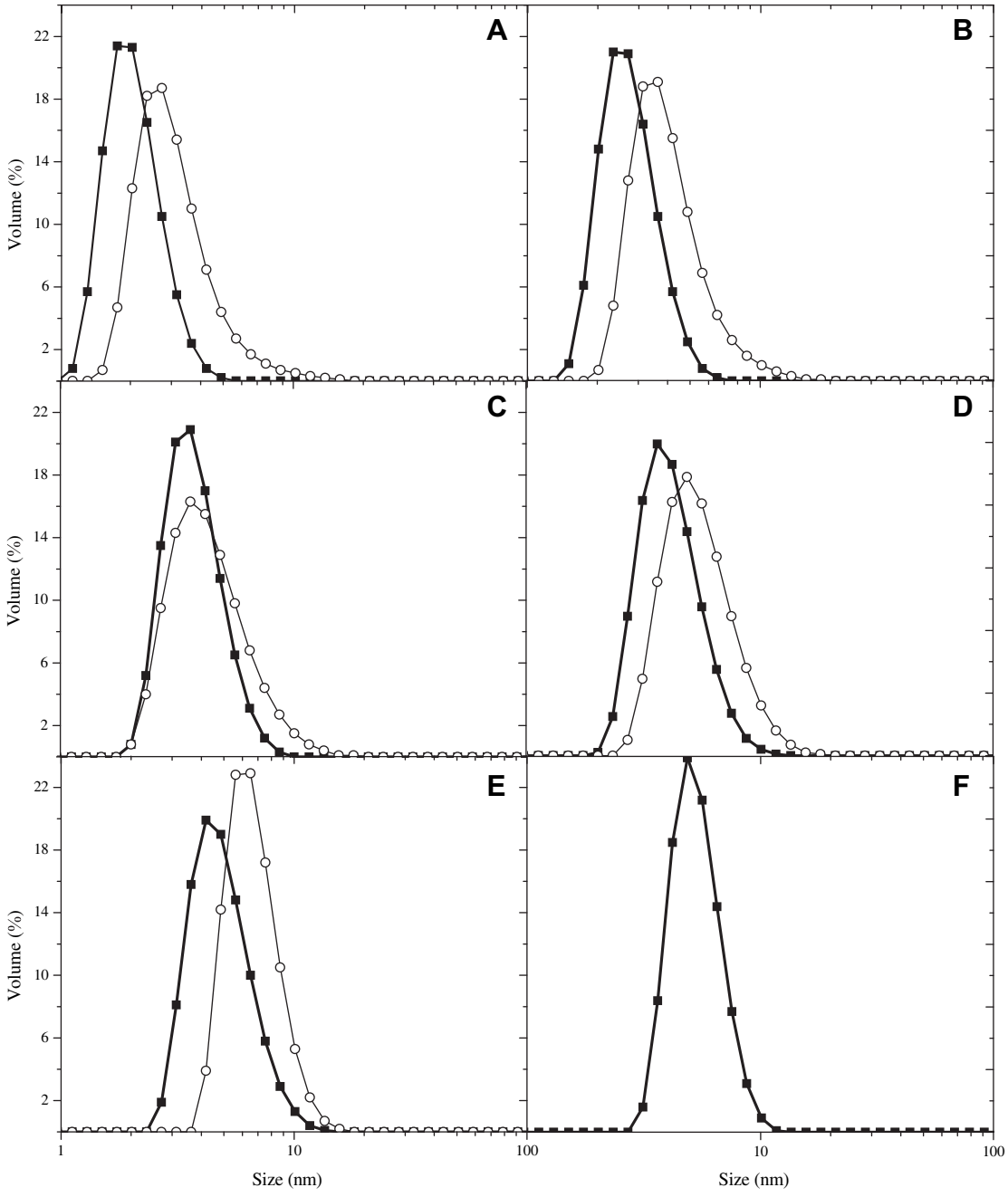

Fig. 4. Volume size distribution at 25 °C for CMP solutions at 5% (w/w) (■) A and (○) B immediately after pH adjustment: (A) pH 6.5; (B) pH 5.5; (C) pH 5; (D) pH 4.5; (E) pH 3.5 and (F) pH 3.

that the CMP-β-lg mixed systems (Martínez et al., 2009) presented a monomodal distribution similar to the β-lg distribution. The intensity of the peak corresponding to large CMP aggregates (100 nm) almost disappeared (Fig. 2) and the peak for the predominant monomeric form of CMP was no longer present in the mixtures. DSC studies of these mixtures indicated the formation of CMP/β-lg complexes driven by electrostatic interactions and/or by hydrogen bonding (Martínez et al., 2009). Thus, the absence of the monomeric form in B CMP solution can be attributed to complex formation between CMP and β-lg.

3.3. Effect of decreasing pH on CMP self-assembly

Due to the effect on the net surface charge, the pH has a major influence on peptide–peptide interactions (Kreuβ et al., 2009) and hence on the particle size intensity distribution of CMP immediately after pH adjustment (Fig. 3). The hydrodynamic diameter of the predominant lower size peak of A CMP size distribution increased to higher sizes when decreasing the pH from 6.5 to 3. Additionally, the peak corresponding to more aggregated forms (100–150 nm) in Fig. 3 was present at most pH values in both CMP preparations (5%, w/w), but their number was negligible as can be deduced from the volume size distribution plots in Fig. 4. Thus most of the particles in both CMP preparations had sizes lower than 10 nm. Similar intensity size distributions were observed for 3 and 5% (w/w) concentrations, reaching maximum values of the lower size peak, of about 6.5 nm, at pH 3–3.5. The maximum of the predominant lower size peak, at pH above 6, was almost constant at around 2.5 nm (Fig. 5). In accordance with the molecular mass estimation by the Zetasizer Nano-Zs software, the increased peak

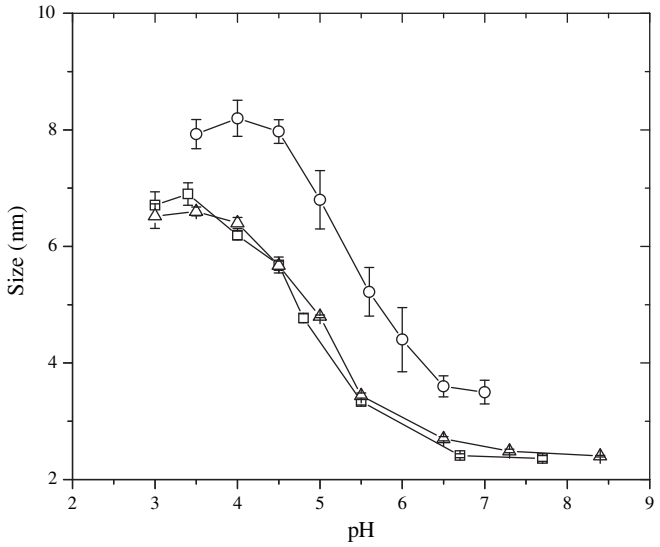

Fig. 5. Size of the predominant lower size peak (from the intensity size distribution by dynamic light scattering) at 25 °C for CMP solutions at concentrations: (□) 3% (w/w) and (△) 5% (w/w) from A CMP and (○) 5% (w/w) from B CMP as a function of pH. Error bars: standard deviation ($n = 3$).

sizes at pH below 6, in Fig. 5, could correspond to CMP self-assembled forms like dimers, tetramers, hexamers and other oligomers. In B CMP solutions it was also observed that the maximum values of the lower size peak increased to 8 nm with decreasing pH to 3.5 but, due to the presence of other contaminant proteins, no estimation of molecular mass could be attempted. The monomeric form was not apparent over the entire pH range (3–7) studied (Figs. 3 and 5).

3.4. Time-dependent self-assembly of CMP

The mean diameter (z-average) immediately after adjusting pH ($t = 0$) showed a minimum at pH 4.5 and a maximum at pH 7 for both, A (Fig. 6) and B (not shown) CMP. Nevertheless, the z-average of B CMP was higher than that of A over the entire pH range studied.

CMP solutions at pH below 4.5 (strongly acidic conditions) showed a time-dependent self-assembly at room temperature, with increasing rates as pH decreased from 4.5 to 3 and as CMP concentration increased from 3 to 5% (w/w) (Fig. 6). At the lower concentration (3%, w/w) the z-average (Fig. 6A) obtained at pH 3 and 3.5 was similar, which would indicate that the concentration is the restrictive factor of the self-assembly rate. CMP aggregation at pH 3.5 has been reported by Wang (2007) who studied a similar CMP sample by differential scanning calorimetry (DSC). A CMP at pH 7 did not show any thermal transition (Martínez et al., 2009). The absence of an endothermic transition (denaturation) is because of its random coil structure (Ono, Yada, Yutani, & Nakai, 1987) and to the absence of disulfide bonds. However, at pH 3.5 an exothermic peak in DSC thermograms was found that was attributed to CMP aggregation (Wang, 2007). However, both studies agree with DLS results discussed above showing CMP aggregation only at pH below 4.5.

Fig. 7A shows, as an example, the evolution of the particle size intensity distribution of A CMP at pH 4 over time at room temperature. It is possible to observe that the predominant lower size peak decreased its intensity and aggregated forms of size higher than 200 nm were formed over time, which accounts for the increase of the z-average shown in Fig. 6. The number of these aggregates was negligible as shown by the volume size distribution plot (Fig. 7B). Nevertheless, the predominant lower peak moved to higher sizes with time, indicating the progress of CMP self-assembly.

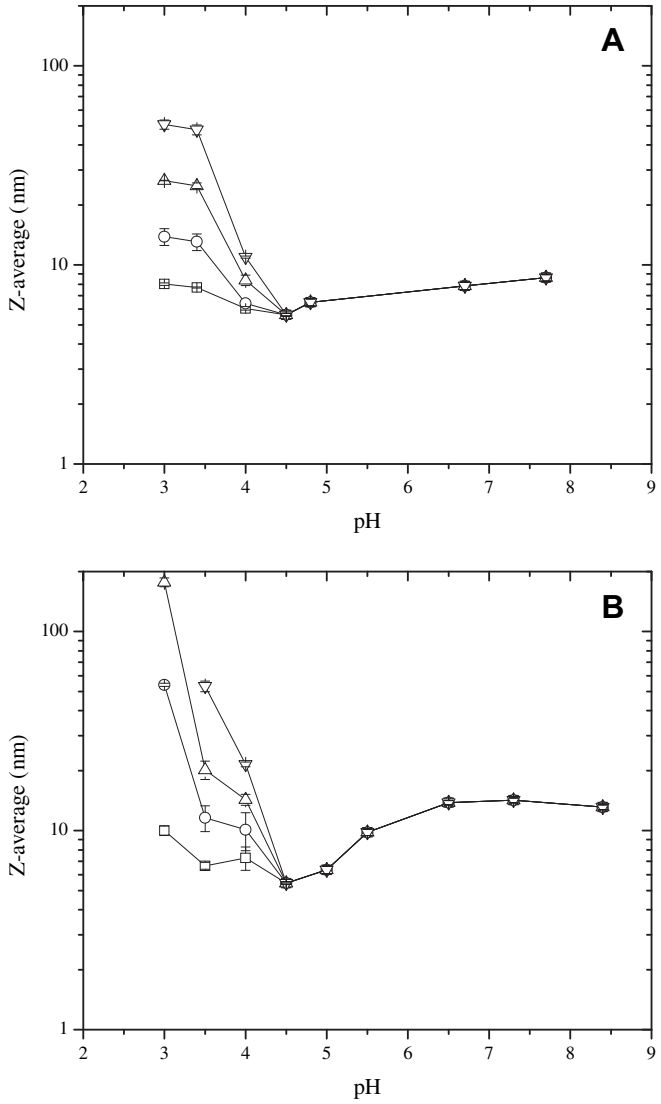

Fig. 6. Z-average as a function of pH over time at 25 °C: (□) 0 min, (○) 20 min, (△) 40 min, (▽) 60 min for A CMP solutions at concentrations (A) 3% (w/w) and (B) 5% (w/w). Error bars: standard deviation ($n = 3$).

3.5. Long-term self-assembly of CMP leading to gelation

As a result of the spontaneous pH-driven self-assembly of CMP at room temperature, the solutions at pH below 4.5 gelled with time. The gels formed were opaque. In Fig. 8 the gelation time (t_{til}) for CMP solutions at concentrations between 3 and 10% (w/w) at pH 3, 3.5 and 4 is plotted. It can be seen that the minimum CMP concentration for gelation was pH-dependent. At pH 3 or 3.5 CMP gelled at concentrations as low as 3% (w/w), however, the times needed for gelation were as long as 150–370 h. At this concentration the solution at pH 4 did not gel, but a precipitate was observed over time (21 days). At pH values higher than 4, gelation was not observed. When CMP concentration was higher than 7–8% (w/w), the gelation time was shorter (<50 h) than for lower concentrations and was almost constant. Only a few studies may be found in the literature on CMP gelation. Recently, Wang (2007) reported that CMP formed a gel in an acidic environment (pH < 4). Burton and Skudder (1987) reported the gelation of a 9.3% (w/w) CMP solution at pH 4.5 and 20 °C, which does not agree with the present study where no gelation was observed at this pH.

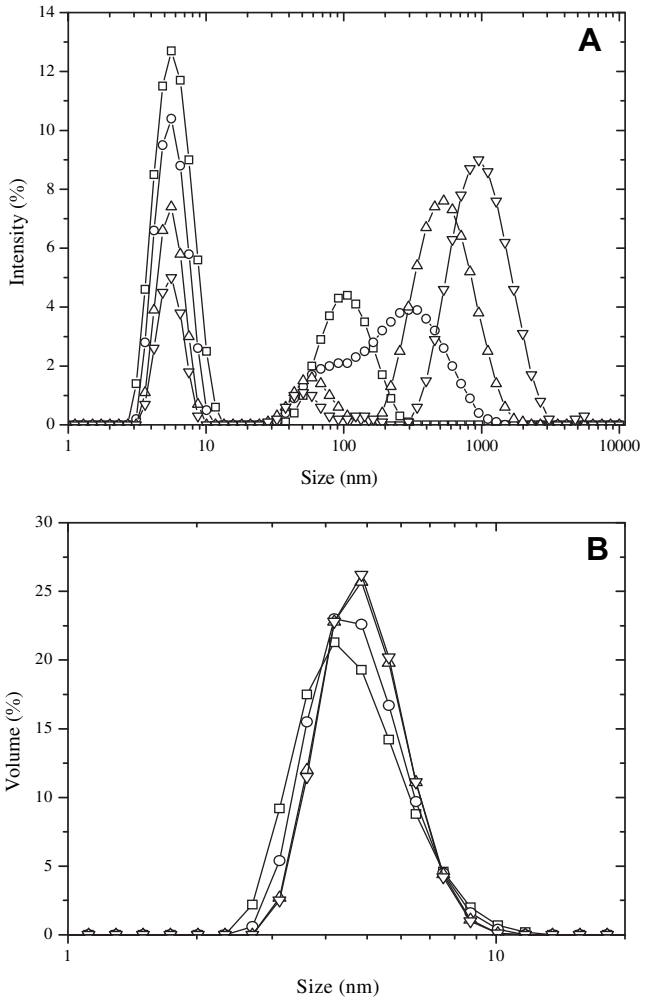

Fig. 7. Intensity (A) and volume (B) size distributions at 25 °C of A CMP solutions (5%, w/w) at pH 4 over time: (□) 0 min; (○) 30 min; (△) 60 min; (▽) 150 min.

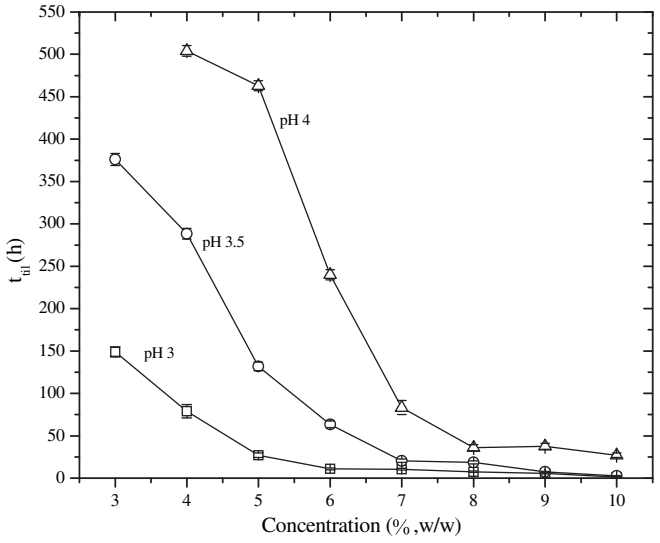

Fig. 8. Gelation time (t_{til}) at 25 °C as a function of pH for A CMP in the range of concentration from 3 to 10% (w/w): (□) pH 3.0; (○) pH 3.5; (△) pH 4.0. Error bars: standard error ($n = 2$ or 3).

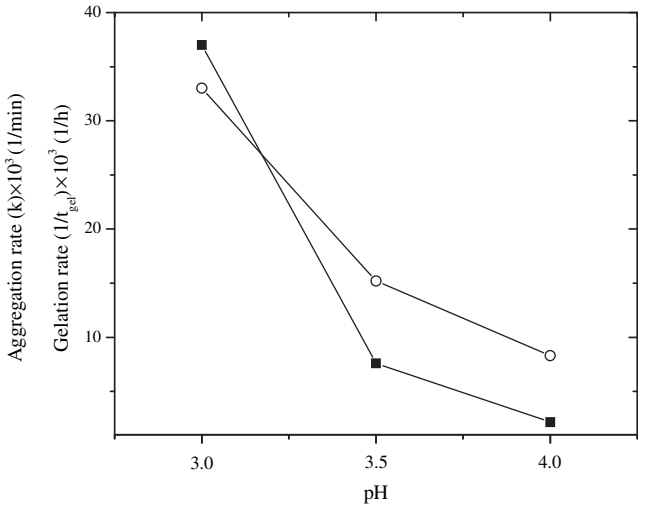

Fig. 9. (○) Initial aggregation rate (by dynamic light scattering) and (■) gelation rate (by the tilting test) as a function of pH at 25 °C for A CMP 5% (w/w).

The relationship between the self-assembly and gelation rate is shown in Fig. 9. The self-assembly rate is the slope of the linear fit (linear regression, LR = 0.99) of the log (z-average) versus time plotted from the results of Fig. 6. The gelation rate, calculated as $1/t_{til}$, showed a strong increase as the pH was lowered from 4 to 3, as the self-assembly rate did, indicating that the gelation was strongly correlated to CMP self-assembly.

3.6. Testing pH-reversibility of self-assembled CMP

The self-assembled CMP was tested for pH-reversibility. In Fig. 10A the z-average of CMP following pH adjustments, from 7 to 3.5 and back to 7 is plotted over time. The z-average of CMP solution at 3% (w/w) at pH 7 was 8 nm. After adjusting the pH to 3.5, the z-average strongly increased over time (from minute 10 to 50) due to the CMP self-assembly. When the pH 7 was restored (50 min after starting the experiment) the z-average decreased rapidly until reaching a z-average slightly higher than the initial one. As can be seen in the size distribution plots by intensity (Fig. 10B) the size distributions before and after the experiment did not coincide. The size distributions of CMP presented three populations. The maximum of the predominant lower size peak moved from about 2.3 to 3.6 nm, which roughly corresponds to the monomeric and dimeric forms of CMP, respectively. The size displacement of the predominant lower size peak was also observed in the volume size distribution (Fig. 10C). These results would indicate that reversibility of self-assembled CMP is not total as the monomeric form is not completely regained after promoting CMP association by pH adjustment.

3.7. CMP self-assembly model

Based on our results and from previous studies (Kreuβ et al., 2008; Kreuβ et al., 2009) a model to explain CMP self-assembly and the formation of a network-like structure (gel) at room temperature is proposed. Fig. 11 shows a scheme of the theoretical pH-dependent self-assembly of CMP.

Among the different side chain interactions that can promote CMP self-assembly and gelation, the covalent bonds formation through the oxidation of sulphydryl groups on cysteine residues is not possible due to the lack of cysteine. Mikkelsen et al. (2005) showed the absence of covalently linked CMP in various size-exclusion chromatography (SEC) fractions of CMP from pepsin-hydrolyzed

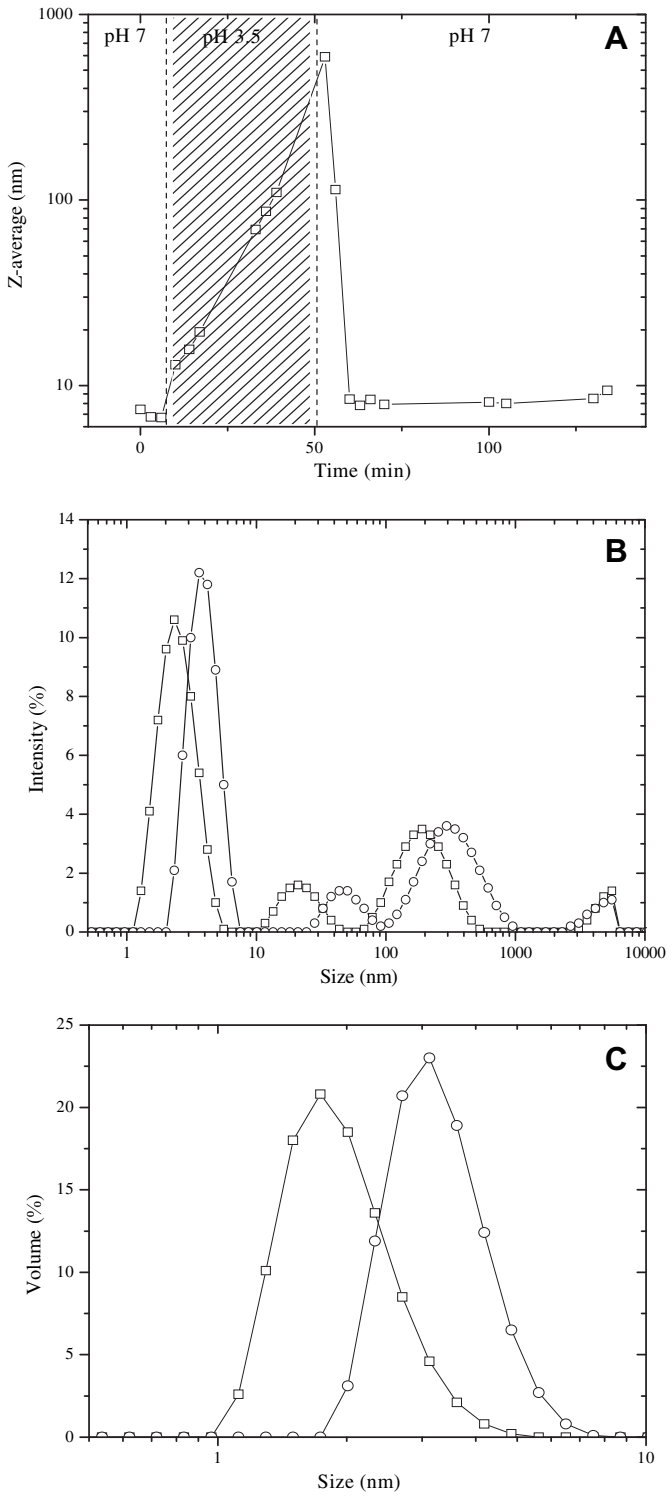

Fig. 10. (A) Z-average as a function of time at 25 °C for A CMP solution at 3% (w/w) with change of pH from 7 to 3 and then returning to 7, (B) intensity and (C) volume size distribution for (□) before and (○) after the test of reversibility brought about by pH adjustment.

κ-casein. However, electrostatic, hydrophobic interactions and hydrogen bonding can take place.

CMP is considered to be affected by changing pH as it contains two Asp, seven or eight Glu (depending on the genetic variant), one phospho-Ser and three Lys residues. Below the isoelectric point (pI), the CMP molecules lose the negative charge of the Glu and Asp residues as well as the carboxyl group at the C-terminus and the sialic acid residues in gCMP. The pI of aCMP is close to 4.1, which is related to the high amount of acidic AA side chains. The positive charge of aCMP at pH levels lower than the pI originates from the three Lys residues as well as from the positively charged N-terminus, while all Glu and Asp residues are protonated. The pI of gCMP, in contrast, is at 3.15, as the negative charge of the sialic acid residues (pK of sialic acid: 2.2) reduces the net charge of the amino acid backbone (Kreuβ et al., 2009).

Most of the hydrophobic domains of CMP (AA1–5, 17–22, 35–39 and 58–65) are masked by the strong charge density of the Glu and Asp residues over a wide range of neutral and basic pH for both fractions, therefore the hydrophobic domains cannot interact. This effect is more pronounced for g CMP due to the negative charge of the terminal sialic acid residues. As shown by Kreuβ et al. (2009), above pH 6.5 when all acidic AA side chains are deprotonated, the zeta potential remains relatively stable at approximately −20 mV for aCMP and −30 mV for gCMP. Thus, above pH 6.5, CMP self-association would be prevented due to the shielding by the strong negative charge, which is more pronounced for gCMP, keeping the monomeric form of CMP predominant (Fig. 2).

Decreasing the pH below 6.5, there is a strong increase of the zeta potential up to the pI (Kreuβ et al., 2009) because of increasing protonation of acidic AA side chains. Therefore the shielding by the negative charges starts to decrease, allowing the N-terminal hydrophobic domain (AA 1–5) which is not covered by the negative charge, to interact first, followed by the hydrophobic domains located in the centre of the peptide chain.

Thus, the first stage of CMP self-assembly to form dimers would occur via pH-driven strong interactions of hydrophobic domains at values below 6.5 (Fig. 11). Once formed, these structures are stable to pH changes.

The test of pH-reversibility of self-assembled CMP by moving the pH back to values above 4.5 (Fig. 10) is in accordance with the proposed model. Moreover, DLS results have shown that the dimeric form of CMP, once formed, by decreasing pH below 6.5 is stable to pH changes. This reveals a strong interaction of hydrophobic domains occurring below this pH. The stability of dimeric forms of CMP have been previously reported by Mikkelsen et al. (2005) that reported associated forms of 35, 18 and 9 kDa at pH 3.4 using SEC. Considering that the Mw of CMP is approximately 7 kDa, Mikkelsen et al. (2005) concluded that CMP exists as tetramers, dimers and monomers. However, SDS–PAGE analysis of the SEC fractions revealed that they could be reduced to a 18 kDa protein band suggesting that dimeric CMP is resistant to dissociation, so they suggested that it is composed of two tightly associated CMP monomers linked by hydrophobic bonds.

A second stage of self-assembly by electrostatic interactions would occur below pH 4.5 between aCMP dimers with a net positive charge and negatively charged gCMP (Fig. 11).

One of the genetic variants of aCMP is less acidic than the other, being uncharged at around pH 4.3–4.6. Only at pH 4.0–4.1 all aCMP is uncharged, whereas gCMP retains a net negative charge due to sialic acid residues. As reported in the literature, gCMP has a heterogeneous composition with increasing amounts of phosphate groups and glycans, especially the highly charged sialic acid (Kreuβ et al., 2008). Five different O-glycans, which are covalently bound to threonine residues or serine, have been identified (Holland, Deeth, & Alewood, 2006). In most cases, the highly negatively charged sialic acid is the terminal carbohydrate.

Decreasing pH below 4, less acidic gCMP isoforms reach their isoelectric state, and at pH 3.15 all gCMP is in the isoelectric state (Kreuβ et al., 2009). Nevertheless, because of the low pK of sialic acid residues (2.2) local negative charges would be located on the glycan down to pH 2.2, allowing it to interact with positive charges.

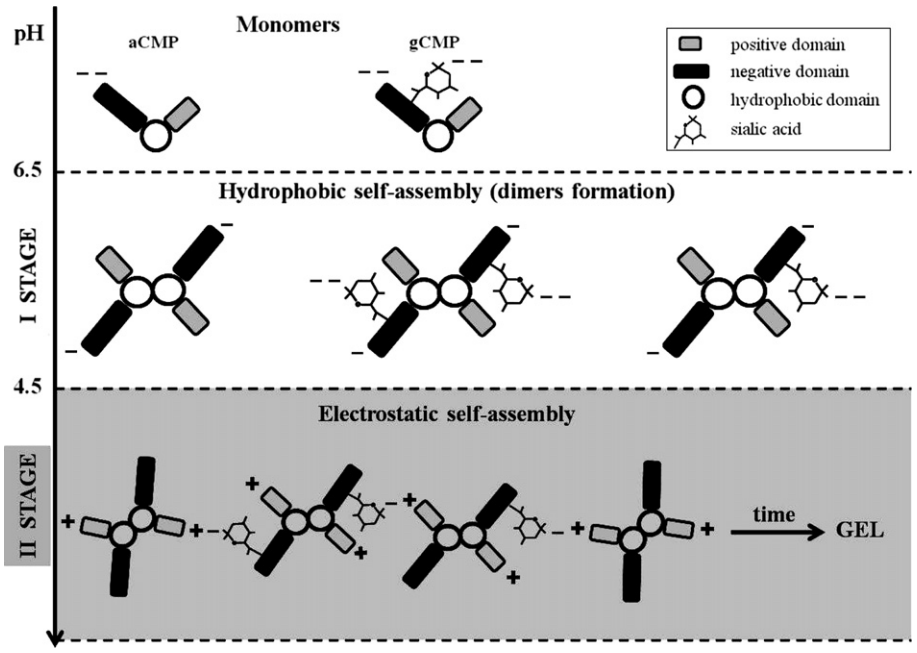

Fig. 11. Scheme of the model proposed to explain the theoretical pH-dependent self-assembly of CMP and the formation of a network-like structure (gel) at room temperature.

Thus in the pH range 2–4.5 the self-assembly via electrostatic bonds can proceed (Fig. 6) to form gel structures over time as shown in Fig. 8.

4. Conclusions

The results reported in this work have shown that CMP undergoes a pH-dependent self-assembly at room temperature. Different self-assembled structures form over time at pH values less than 4.5, and at certain CMP concentrations, form gels. Self-assembled structures are partially pH-reversible, but dimers appear to be resistant to pH changes once formed.

CMP self-assembly would include a first stage of hydrophobic self-assembly to form dimers which further interact through electrostatic bonds to form gels over time. In the proposed model, it is evident that the second stage of self-assembly that leads to gelation is only possible in the presence of glycan side chains, mainly sialic acid, which retains negative charges down to pH 2.2. Thus the presence of charged glycosidic side chains is of huge importance in determining the techno-functional properties of CMP, which deserves future studies.

Acknowledgements

This research was supported by Universidad de Buenos Aires, Universidad Nacional de Luján, Agencia Nacional de Promoción Científica y Tecnológica and Consejo Nacional de Investigaciones Científicas y Técnicas de la República Argentina.

References

Baeza, R. I., Gugliotta, L. M., & Pilosof, A. M. R. (2001). Heat induced aggregation of β-lactoglobulin in the presence of non gelling polysaccharides studied by dynamic light scattering. *Proceedings of EMPROMER 2001, III*, 1513–1518.

Burton, J., & Skudder, P. J. (1987). *Whey proteins*. UK patent Application GB 2188526 A1.

Bollag, D. M., & Edelstein, S. J. (1991). Gel electrophoresis under denaturing conditions. In D. M. Bollag, & S. J. Edelstein (Eds.), *Protein methods* (pp. 95–141). New York, NY, USA: Wiley-Liss, Inc.

Cherkaoui, S., Doumenc, N., Tachon, P., Neeser, J. R., & Veuthey, J. L. (1997). Development of a capillary zone electrophoresis method for caseinoglycomacropeptide determination. *Journal of Chromatography A, 790*, 195–205.

Coolbear, K. P., Elgar, D. F., & Ayers, J. S. (1996). Profiling of genetic variants of bovine κ-casein macropeptide by electrophoretic and chromatographic techniques. *International Dairy Journal, 6*, 1055–1068.

Daali, Y., Cherkaoui, S., & Veuthey, J. L. (2001). Capillary electrophoresis and high-performance anion exchange chromatography for monitoring caseino-glycomacropeptide sialylation. *Journal of Pharmaceutical and Biomedical Analysis, 24*, 849–856.

Elofsson, U., Dejmek, P., & Paulsson, M. (1996). Heat-induced aggregation of β-lactoglobulin studied by dynamic light scattering. *International Dairy Journal, 6*, 343–357.

El-Salam, A. M. H., El-Shibiny, S., & Buchheim, W. (1996). Characteristics and potential uses of the casein macropeptide. *International Dairy Journal, 6*, 327–341.

Etzel, M. R. (1999). *Production of κ-casein macropeptide for nutraceutical uses*. U.S. Patent 5,968,586.

Guyomarc'h, F., Nono, M., Nicolai, T., & Durand, D. (2009). Heat-induced aggregation of whey proteins in the presence of κ-casein or sodium caseinate. *Food Hydrocolloids, 23*, 1103–1110.

Harnsilawat, T., Pongsawatmanit, R., & McClements, D. J. (2006). Characterization of beta lactoglobulin–sodium alginate interactions in aqueous solutions: a calorimetry, light scattering, electrophoretic mobility and solubility study. *Food Hydrocolloids, 20*, 577–585.

Holland, J. W., Deeth, H. C., & Alewood, P. F. (2006). Resolution and characterization of multiple isoforms of bovine kappa-casein by 2-DE following a reversible cysteine-tagging enrichment strategy. *Proteomics, 6*, 3087–3095.

Hoffmann, M., Roefs, S., Verheul, M., Van Mil, P., & De Kruif, K. (1996). Aggregation of β-lactoglobulin studied by in situ light scattering. *Journal of Dairy Research, 63*, 423–440.

Karlsson, A. O., Ipsen, R., Schrader, K., & Ardö, Y. (2005). Relationship between physical properties of casein micelles and rheology of skim milk concentrate. *Journal of Dairy Science, 88*, 3784–3797.

Kawasaki, Y., Kawakami, H., Tanimoto, M., Dosako, S., Tomizawa, A., & Kotake, M. (1993). pH-dependent molecular weight changes of kappa-casein glycomacropeptide and its preparation by ultrafiltration. *Milchwissenschaft, 48*, 191–196.

Kreuβ, M., Krause, I., & Kulozik, U. (2008). Separation of a glycosylated and non-glycosylated fraction of caseinomacropeptide using different anion-exchange stationary phases. *Journal of Chromatography A, 1208*, 126–132.

Kreuβ, M., Strixner, T., & Kulozik, U. (2009). The effect of glycosylation on the interfacial properties of bovine caseinomacropeptide. *Food Hydrocolloids, 23*, 1818–1826.

Laemmli, U. K. (1970). Cleavage of structural proteins during the assembly of head of bacteriophague T4. *Nature, 227*, 680–687.

Lieske, B., Konrad, G., & Kleinschmidt, Th (2004a). Isolation of caseinomacropeptide from rennet whey by a multi-stage ultrafiltration process. I. Studies in the apparent molecular weight of caseinomacropeptide as a function of pH. *Milchwissenschaft, 59*, 172–175.

Lieske, B., Konrad, G., & Kleinschmidt, Th (2004b). Isolation of caseinomacropeptide from rennet whey by a multistage ultrafiltration process. III. Influence of pH in the first ultrafiltration-step on the chemical properties of isolated caseino-macropeptide. *Milchwissenschaft, 59*, 408–410.

Martínez, M. J., Carrera Sánchez, C., Rodríguez Patino, J. M., & Pilosof, A. M. R. (2009). Interactions in the aqueous phase and adsorption at the air–water interface of

caseinoglycomacropeptide (GMP) and β-lactoglobulin mixed systems. *Colloids and Surfaces B: Biointerfaces, 68*, 39–47.
McGuffey, M. K., Otterb, D. E., van Zantenc, J. H., & Foegeding, E. A. (2007). Solubility and aggregation of commercial α-lactalbumin at neutral pH. *International Dairy Journal, 17*, 1168–1178.
Mehalebi, S., Nicolai, T., & Durand, D. (2008). Light scattering study of heat-denatured globular protein aggregates. *International Journal of Biological Macromolecules, 43*, 129–135.
Mikkelsen, T., FrØkiœr, C., Topp, C., Bonomi, F., Iametti, S., Picariello, G., et al. (2005). Caseinomacropeptide self-association is dependent on whether the peptide is free or restricted in k-casein. *Journal of Dairy Science, 88*, 4228–4238.
Mollé, D., & Leonil, J. (2005). Quantitative determination of bovine κ-casein macropeptide in dairy products by liquid chromatography/electrospray coupled to mass spectrometry (LC–ESI/MS) and liquid chromatography/electrospray coupled to tandem mass spectrometry (LS–ESI/MS/MS). *International Dairy Journal, 15*, 419–428.
Morr, C., & Seo, A. (1988). Fractionation and characterization of glycomacropetide from caseinate and skim hydrolysates. *Journal of Food Science, 53*, 80–87.
Nakano, T., Ikawa, I., & Ozimek, L. (2007). Detection of sialylated phosphorylated κ-casein glycomacropeptide electrophoresed on polyacrylamide gels and cellulose acetate strips by the thiobarbituric acid and malachite green dye reactions. *Journal of Agricultural and Food Chemistry, 55*, 2714–2726.
Nakano, T., & Ozimek, L. (1998). Gel chromatography of glycomacropeptide (GMP) from sweet whey on Sephacryl S-200 at different pH's and Dephadex G-75 in 6 M guanidine hydrochloride. *Milchwissenschaft, 53*, 629–633.
Nakano, T., & Ozimek, L. (2000). Purification of glycomacropeptide from dialyzed and non-dialyzable sweet whey by anion-exchange chromatography at different pH values. *Biotechnology Letters, 22*, 1081–1086.
Ono, T., Yada, R., Yutani, K., & Nakai, S. (1987). Comparison of conformations of κ-casein, para-κ-casein and glycomacropeptide. *Biochimica et Biophysica Acta, 911*, 318–325.
Relkin, P., Meylheuc, T., Launay, B., & Raynal, K. (1998). Heat-induced gelation of globular protein mixtures. A DSC and scanning electron microscopic study. *Journal of Thermal Analysis, 51*, 747–755.
Roefs, S., & De Kruif, K. (1994). A model for the denaturation and aggregation of β-lactoglobulin. *European Journal Biochemistry, 226*, 883–889.
Semenova, M. G. (2007). Thermodynamic analysis of the impact of molecular interactions on the functionality of food biopolymers in solution and in colloidal systems. *Food Hydrocolloids, 21*, 23–45.
Sharma, M., Haque, Z. U., & Wilson, W. W. (1996). Association tendency of beta lactoglobulin AB purified by gel permeation chromatography as determined by dynamic light scattering under quiescent conditions. *Food Hydrocolloids, 10*, 323–328.
Silva-Hernández, E., Nakano, T., & Ozimek, L. (2002). Isolation and analysis of κ-casein glycomacropeptide from goat sweet whey. *Journal Agricultural and Food Chemistry, 50*, 2034–2038.
Silva-Hernández, E., Nakano, T., Verdalet-Guzmán, I., & Ozimek, L. (2004). Comparison of glycomacropeptide isolated from raw and pasteurized goat milk. *Milchwissenschaft, 59*, 27–31.
Stepanek, P. (1993). Data analysis in light scattering. In W. Brown (Ed.), *Dynamic light scattering. The methods and some applications* (pp. 177–241). London, UK: Clarendon Press.
Thomä-Worringer, C., Sørensen, J., & López Fandiño, R. (2006). Health effects and technological features of caseinomacropeptide. *International Dairy Journal, 16*, 1324–1333.
Tolkach, A., & Kulozik, U. (2005). Fractionation of whey proteins and caseinomacropeptide by means of enzymatic crosslinking and membrane separation techniques. *Journal of Food Engineering, 67*, 13–20.
Wang, Q. (2007). *Application of low-intensity ultrasound to characterise the microstructure of model food systems*. PhD Thesis, Technischen Universität München, Germany.
Wang, T., & Lucey, J. A. (2003). Use of multi-angle laser light scattering and size-exclusion chromatography to characterize the molecular weight and types of aggregates present in commercial whey proteins products. *Journal of Dairy Science, 86*, 3090–3110.